

## PREDICTION AND SIMULATION OF MALAYSIAN FOREST FIRES BY RANDOM SPREAD

**J. Serra<sup>1</sup>, M. d. H. Bin Suliman<sup>2</sup> and M.Mahmud<sup>2</sup>**

<sup>1</sup>Université Paris-Est, Laboratoire d'Informatique Gaspard Monge, Equipe  
A3SI, ESIEE Paris, France

<sup>2</sup> Earth observation centre, Faculty of Geography, UKM, Malaysia

Corresponding Author's E-mail: j.serra@esiee.fr

**Abstract**— The paper aims to study forest fires from risk maps and satellite data, in order to predict the location of the burnt zones they provoke. The approach is based on the discrete stochastic model of a random spread, which describes both fire fronts and burnt areas. Under iteration, it provides the time evolution of the process. The probabilities of spontaneous extinction at each stage are derived. The random spread model is then applied to analyse the fires that occurred in the State of Selangor (Malaysia) from 2001 to 2004. It is used, firstly, to simulate forest fires, according to a law of intensity (fuel combustion) and another of extension (spread rate). But the next, and more important, result lies in the ability of the model to predict all places where burnt scars actually occurred, which turns out to be a significant verification.  
Introduction

### 1. INTRODUCTION

#### 1.1 Forest fires in Southeast Asia

The major vegetation fires in Southeast Asia during the El Nino event of 1997 triggered a worldwide interest due to its massive environment disaster when a blanket of thick, brown haze enveloped much of Southeast Asia. The cause of the haze was due to the forest and bush fires that lasted several months, deliberately lit by farmers to clear land for oil palm plantations in Sumatra and the development of the 'mega rice' project in Kalimantan, Indonesia, magnified by the drought brought by the El Nino phenomenon. During the dry periods of strong El Nino of the 1986-1987, 1994 and 1997-1998, an estimate of 3.5 million hectares, 4.5 million hectares and 9.5 million hectares of forest and land were burnt in Indonesia (ADB Bank report, 1999).

The occurrences of forest fires in the natural protected forests of Peninsular Malaysia are generally low, but are more frequent in the secondary forests, peat swamp forests, and forest plantations (Abdullah *et al.* 2002). Peninsular Malaysia still retains approximately 5.97 million hectares of natural forest that mainly consists of 89% of dipterocarp forests, which constitutes 45.4% of the land areas (Qiang and Braodhead, 2002). Most of the

forest fires in Malaysia take place during the dry spells from January to March, and from June to August (Gantz, 2002). However, incidences of uncontrolled forest fires have been increasing since 1991 as a result of land clearing activities that involve open burning due to human negligence or uncontrolled fires that encroach into the neighboring forestland and for cultivation in peat forests (Maarof, 2002). A total of 35 cases of forest fires were reported from 1991 to 2002 that covered 4,143 hectares (ADB Bank report, 1999).

The land use in Selangor is mainly composed of oil palm plantation, peat swamp forest, plantation forest, inland forest, scrub, urban area and ex-mining areas. The fires occur mainly in the peat swamp forest, beris (heath) forest and bush areas (Mahmud 1999; Wan Ahmad 2002). They spread slowly through the thick peat layers, making their detection and extinction difficult. From 1995 to 2005, fires occurred in Kuala Lumpur, Sg. Karang and Raja Muda Reserve Forest, Selangor. Most of them were caused by human activities; some were due to carelessness or burning activities.

## **1.2 Objectives**

When one considers a forest fire which has started, several questions about its future can be formulated, such as:

- 1/ will the fire still spread after one or two days, or more, and in which directions?
- 2/ can we predict the long-term extension of the burnt zone, or scar, where long-term may mean several dry seasons?

The first question concerns the burning process, and involves the front of the spread, whereas the second deals with the final result of the phenomenon. In this paper, we intend to formulate both questions in the framework of a stochastic model, and to apply it to the second question. A natural fire propagation is not fully predictable, and the part of randomness it involves can be interpreted by restricting the evolution of fire spread to a few random secondary seats. The basic hypothesis of this paper is that such a level of randomness is sufficient to formulate the two above questions. The corresponding theory is presented in Sections 3 and 4.

In Section 5, the theory is applied to forest fires of the State of Selangor, in Malaysia, (Figure 1). However, the material available in this study for locating the burnt zones, as presented in Section 2.3, allows us to validate the model for its long term predictions only. Indeed, in the maps of hot spots to which we refer, the pixel size equals 1km × 1km, which makes impossible to detect fine daily variability. Therefore the question of short term forecast, by means of the induction relation (6), will not be treated here.

## **1.3 State of the art**

The literature about quantitative modelling of Canadian, Malaysian, Mediterranean, U.S. or Australian forest fires, can be split into two groups. Firstly, the behaviour of a forest fire is often described from what is actually observed (Carrega, 2002; Wan 2002). Pertinent parameters are defined from permanent sources (fuel maps, soil nature) or from other variables (typically weather observations such as temperature, relative humidity,

wind, rain) (Canadian Forestry, 1992). Complex systems have been proposed for managing this information, which result in behaviour predictions of the rate of spread, of the fuel consumption, of the temperature at the front of the fire, etc. (Blanchi and Al. 2002; Colin and Al. 2002). Their predictions yield daily maps which are often synthesized in an overall risk map. Such descriptions incorporate the satellite data, for land cover classification and the associated hot spots.



Figure 1: map of Peninsular Malaysia and the state of Selangor. The figure also shows the distribution of the automatic weather stations in Peninsular Malaysia.

Although these descriptions are quantitative, the heart of the description lies in the differential equations that underlay a fire. Several phenomena are involved, such as heat transfer, gas properties (Catchpole, 2002), or turbulence phenomena, annihilation of opposite fires (Bak and Al. 2001), or again irreversible thermodynamics (Sero-Guillaume and Margerit, 2002) etc. Such physical analyses go to the core of fire modelling.

The gap between the two approaches is understandable. The use of the Navier-Stokes partial differential equation (PDE) in (Sero-Guillaume and Margerit, 2002), for example, requires that the elementary turbulences exactly fulfil this differential equation, which is obviously not the case when a pine cone is suddenly projected at 300 metres, and provokes a new seat of fire. Such a physical model focuses on one aspect of the reality in order to draw derivations about this exclusive side. But there are a number of other aspects, e.g. the wind, the moisture, the slope of the ground, the recent past, the underground propagation (in peat swamp forests), etc. (Canadian Forestry, 1992). All these

factors interfere when an actual fire propagates, making the practical use of one specific physical PDE extremely difficult.

A contrario, this practical impossibility explains and justifies the heuristic approaches by spread maps, fuel maps, and risk maps. Even if they are not always dimensionally consistent, these maps, which concentrate a lot of information and experience, remain precious indexes. The same impossibility leads us to replace the deterministic physical PDE's by the probabilities of fire propagation, via a random model.

## 2. MATERIAL

The three pieces of information we shall use below as parameters for the random spread model are, firstly, satellite observations of "hot spots", plus two GIS raster maps that describe the potential extension and intensity of a fire. Form these three elements, and some assumptions, the model establishes a predictive map of the burnt areas, which can be compared with the actual scars, or burnt areas. This map of the scars is therefore the four and last information required.

### 2.1 Hotspots

Hot spots are defined as those image pixels whose brightness temperatures exceed a pre-defined threshold value. Threshold values of 316 to 320 K have been reported in scientific literature, encompassing a range of high temperature bodies including forest and vegetation fires. In this study, we focus on the hot spots in the state of Selangor, during the period 2000 - 2004, and which are detected by sensor of the National Oceanic Atmospheric Administration satellite NOAA, Advanced Very High Resolution Radiometer (AVHRR). The sizes of the image pixels, for this satellite, vary approximately from 1.1 by 1.1 km at the nadir, to almost 4 km by 1.1 km on the outer edge of the track (CRISP, 2001). The satellite provides infrared images whose digital values range from 0 to 1023. The cumulative number of hot spots from 2000 to 2004, during the three periods April-June, July-September, and October-December, are depicted in Figure 2a, b, and c (for the sake of display, the "points" appear as small rhombs, but they are treated as actual points in all computations).

### 2.2 The two GIS raster maps

#### 2.2.1 Spread rate map

The Initial Spread Index (ISI) is a measure of the expected rate of fire spread. Its spatial variation generates the so-called "Spread rate map". It is obtained by the Spatial Fire Management System (sFMS) software, which develops fire science models in a GIS environment. The Initial Spread Index ISI combines the wind speed data  $f(W)$  with the Fine Fuel Moisture Code parameter FFMC according to Van Wagner relation (Van Wagner, 1987) :

$$ISI = 0.208 \times FFMC \times f(W)$$

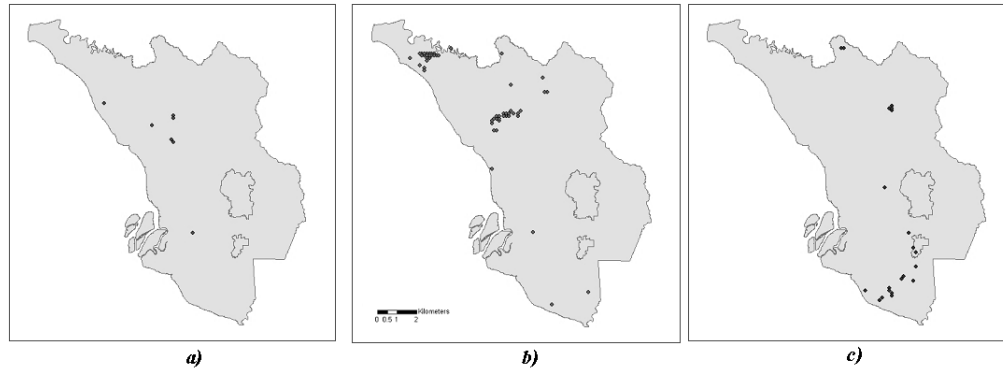


Figure 2: Cumulative number of hot spots from 2000 to 2004, during the periods April-June (a), July-September (b), and October-December (c).

Figure 3 depicts the corresponding flow chart. The FFMC allows us also to estimate a Fire Weather Index (FWI) system components. Inputs to FFMC include elevation and daily weather data. The weather data is retrieved from 24 automatic weather stations, which are operated by the Malaysian Meteorology Services throughout Peninsular Malaysia. The digital elevation model (DEM) for Peninsular Malaysia is drawn from the Shuttle Radar Topography Mission (SRTM), whose data result, after correction, in a resolution of 90 meters. FFMC is used as an indicator of ignition potential for fires to spread in the considered area. Finally, the Initial Spread Index (ISI) combines FFMC and wind speed

The Spread Rate Map of ISI data is calculated on a cell-by-cell basis. Because of the limited weather stations in Peninsular Malaysia and the coarse resolution of the interpolation, this Spread Rate Map only gives a general idea of the spread rate present. The restriction of this map to the State of Selangor is depicted in Figure 4a.

### 2.2.2 Fuel consumption map

The fuel consumption map  $f$  provides an indicator of the propensity of a fire to grow. It directly derives from the map of the vegetal cover depicted in Figure 4b, by multiplying each basic type of vegetation by its own flammable value as reported in Table 1 (SEAFDRS, 2003), which results in the map  $f_w = f.w$  of Figure 4c. The flammable values are obtained by calibration with hot spot data, by using the Zonal Statistical method

Table 1

<i>fuel type f</i>	<i>grey level of Figure3b</i>	<i>area in pixels</i>	<i>flammable value w</i>
urban area	black	2 950	0
primary forest	dark grey	16 479	3

rubber and other	medium grey	34 370	4
oil palm tree	light grey	13 637	4
peat swamp forest	white	12 533	5

(ESRI, 2006)

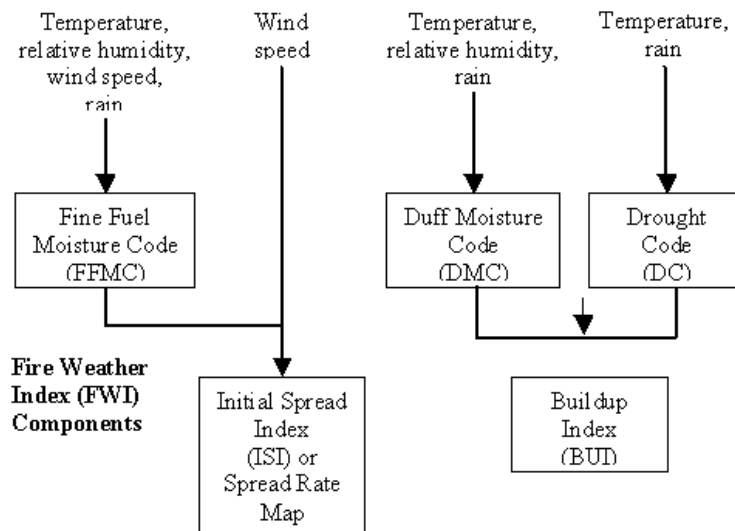


Figure 3: Fire Weather Index (FWI) system components. The map obtained by this system is depicted in Figure 4a.

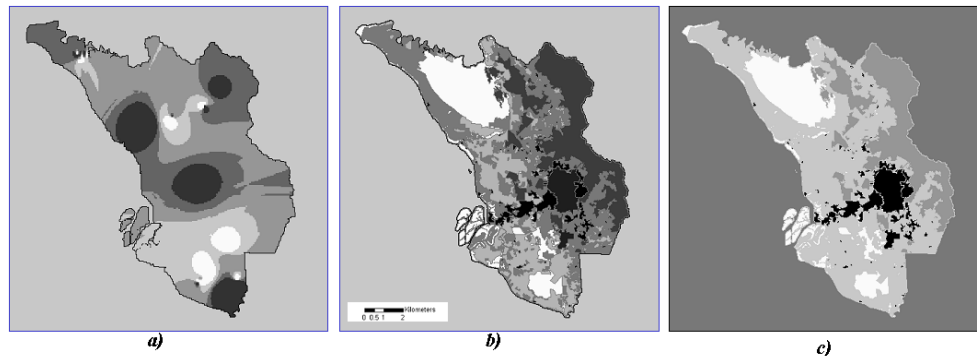


Figure 4: Selangor State. a) Map of the spread rate, i.e. of the radius  $r$  of the daily circular propagation of the fire; b) map  $f$  of the fuel types (the clearest tone corresponds to peat swamp forest); c) map  $f_w$  of the fuel consumption, i.e. a weighted version of Figure 4b according to the weights introduced in Table 1.

### 2.3 Burnt zones, or scars

The word "scar" borrowed from the forestry services, is synonym of "region burnt by fires". The Scar information about the south part of Selangor ( two zones in Figure 6) was provided by the Fire and Rescue Department of Selangor. As for the northern part of the same figure, we directly worked on satellite images, and the burnt scar was obtained by a supervised classification using a knowledge base, followed by a post-classification (the latter takes place after classification for enhancing spatial features, thus increasing its accuracy).

For detecting and assessing the changes of burnt scar over times, three images were used, namely:

- multi-temporal Landsat-TM data of 6 March 1990 (before fire occurrence),

- Landsat-ETM data of 21 September 2001 (Two months after the fire occurrence of 6-9 July 2001),

- SPOT-4 data of 15 March 2005, (one month after the fire occurrence of 14-28 February 2005).

The classified data of Landsat-ETM and SPOT-4 were converted into vector for extracting the boundaries of the burnt scar area. The explicit flow-chart of the methodology is given in Figure 5 (an alternative approach, holding on a more comprehensive data base of forest fires, may be found in (Zhang and Al. 2003).

Figure 6 illustrates in detail the results of this procedure for one of the sub-areas of north Selangor. A Landsat-TM image with a resolution of 30m, taken on March the 6th, 1990, i.e. eleven years before the first forest fires of the period, were compared with the 2001 Landsat-ETM image and with the 2005 SPOT-4 image. The path and row grid equals 127/058 for Landsat (TM and ETM) and 269/343 for SPOT. The satellite SPOT-4

XS has a spatial resolution of 20 metres, and four bands, one of them operating in the mid-infrared wavelength, while Landsat has a spatial resolution of 30 meters and supplies high resolution in visible and infra-red imagery. Thermal imagery and a panchromatic image are also available from the ETM sensor.

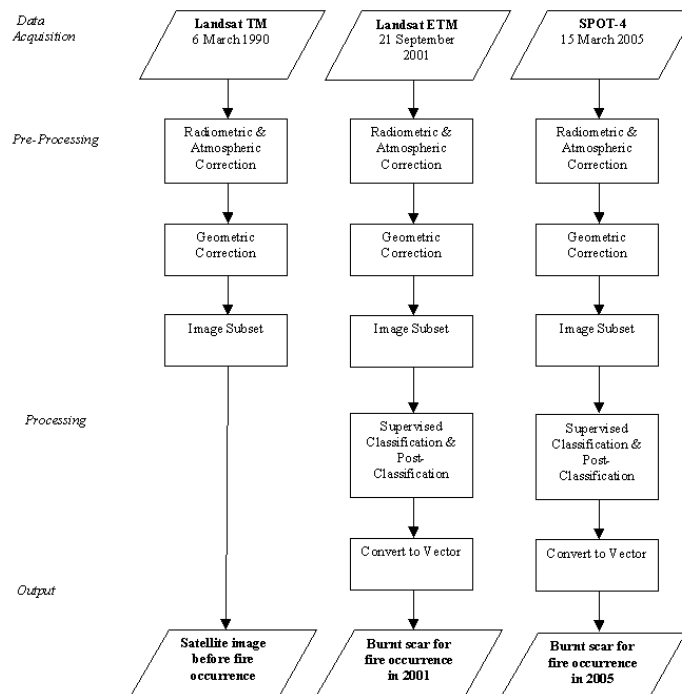


Figure 5: Flow-chart for the detection of burnt scar.

We suppose here that the burnt areas can be identified as such by comparing three images which cover fifteen years. Such a large time interval is needed for finding the cumulated effects of the fires. Now, clearly, the re-vegetation, the conversion to another land use may introduce a bias. But such a bias can only underestimate the scars. When there are present, they are significant, and this information is already important for the model we view.



Figure 6: a) Landsat-TM, 6 March 1990; b) Landsat-ETM, 21 September 2001, i.e. two month after the last forest fires of the period; c) SPOT-4,15 March 2005, i.e. one month after the last forest fires of the period.

### 3. METHOD: THE RANDOM SPREAD MODEL

#### 3.1 Definition

The Random Spread model, introduced below for modelling forest fires spread in the State of Selangor, involves some mathematical derivations which should be cumbersome in this paper. The reader can find them in (Serra 2007). The R.S. model depends on two parameter maps. In its application to Selangor state, the first parameter is given by the spread rate map, as depicted in Figure 4a, and the second parameter is proportional to the fuel consumption map of Figure 4c. We depict in Figure 7 two sub-maps of Figure 4 a and c, that correspond to the exact zone on which R.S. model is illustrated in Figures 8 to 10 below.

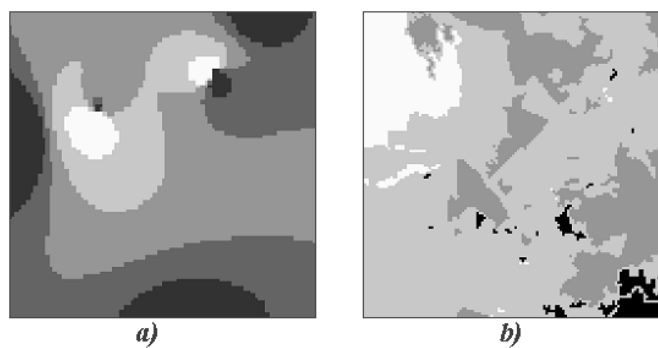


Figure 7: a) and b) Two sub maps showing a central region of Figure 4a and 4c respectively

A random spread is a double discrete process. According to this model, the fire comes at time  $n$  in the form of two sets, denoted by  $X_n$  and  $I_n$ . Set  $X_n$  indicates the zone burnt between times  $n-1$  and  $n$ , and  $I_n$  is the set of point seats, in finite number, that appeared between  $n-1$  and  $n$ . Two such inputs are depicted in Figure 8a and 8b. One goes from the doublet  $(X_n, I_n)$  to the next stage  $(X_{n+1}, I_{n+1})$  by the three following steps:

Set  $X_{n+1}$  is the dilate of  $I_n$  by the so-called function  $\delta$ ; in other words, each seat  $x_i \in I_n$  is replaced by the disc  $\delta(x_i)$  whose radius is given by the value of the spread rate map at point  $x_i$  and the union of all these discs results in  $X_{n+1}$  (Figure 8c)

$$X_{n+1} = \delta(I_n) = \cup \{ \delta(x_i), x_i \in I_n \} ; \quad (1)$$

For each disc  $\delta(x_i)$  involved in Rel.(1), one generates a different realization  $P_i$  of Poisson points, whose variable intensity  $\theta$  is proportional to the fuel map  $f_w$ . Realization  $P_i$  is then intersected with the dilate  $\delta(x_i)$ :

$$[ \delta(x_i) ; P_i ] \Rightarrow \delta(x_i) \cap P_i . \quad (2)$$

The three pictures of Figure 9 depict such realizations and intersections for the three points of seat  $I_n$ ;

Finally, one takes for new seats  $I_{n+1}$  the union

$$I_{n+1} = \beta(I_n) = \cup \{ (\delta(x_i) \cap P_i), x_i \in I_n \} \quad (3)$$

of all those Poisson points that are intersected by the  $\delta(x_i)$ , for  $x_i \in I_n$ .

Relations (1) and (3) express the passage from stage  $n$  to stage  $n + 1$ , and serve in turn as an input for going from stage  $n + 1$  to stage  $n + 2$ . The induction procedure will be completely described when the initial stage is given. It suffices, indeed, to know the initial seat  $I_0$ . Under dilation  $\delta$ ,  $I_0$  generates  $X_1$ , and by applying the above step 2 to all  $\delta(x_i)$ ,  $x_i \in I_0$ , followed by union (3), one generates also  $I_1$ .

Moreover, if  $J$  and  $J'$  are two disjoint point seats whose union give  $I_0$ , then we have

$$I_1 = \beta(I_0) = \beta(J \cup J') = \beta(J) \cup \beta(J') . \quad (4)$$

Since, in the Euclidean plane, Poisson points are always disjoint, the relation (4) of superimposition allows us to reduce the initial seat  $I_0$  to a unique point,  $x_0$  say.

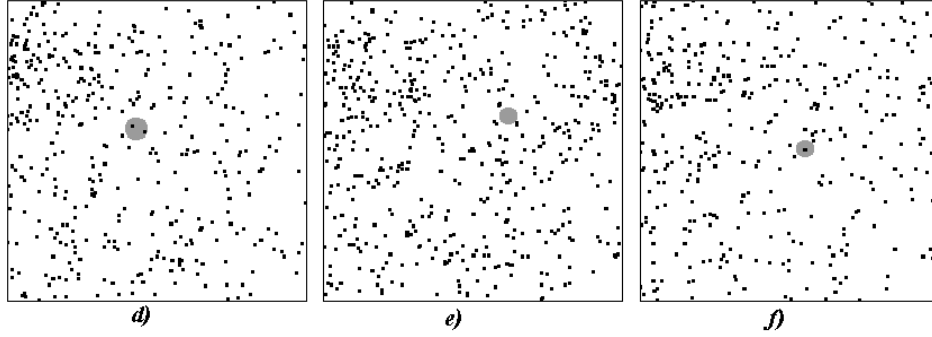


Figure 9: d), e), and g) intersections of each particle of  $X_{n+1}$  with a different Poisson points realization. Note the higher number of Poisson points in the top left parts of the fields.

### 3.2 Characteristic functional

In the Euclidean plane every random closed set  $X$  is characterized by the probabilities

$$Q(K) = \Pr\{K \subseteq X^c\} \quad (5)$$

that compact set  $K$  misses the random set  $X$ , when  $K$  spans the family of all compact sets (Matheron, 1975). The property remains valid in digital space, by changing "compact  $K$ " into "finite  $K$ ". Therefore, for characterizing the  $n^{\text{th}}$  spread  $X_n(x_0)$  of initial seat  $x_0$ , we must calculate the probability  $Q_n(K | x_0)$  that set  $K$  misses  $X_n(x_0)$ . We have that

$$Q_n(K | x_0) = \exp\left\{1 - \int_{\zeta(x_0)} \theta(dy) Q_{n-1}(K | y)\right\} \quad (6)$$

where function  $\zeta$  is the reciprocal of  $\delta$ , i.e.  $\zeta(x) = \cup \{y: x \in \delta(y)\}$ . Relation (6) is exactly right for short term evolution to predict, since it determines the probabilities at time  $n$  from that at time  $n-1$ . This induction relation makes the characteristic functional is easily calculable by successive substitutions. In particular, the first two steps admit the following functionals

$$Q_1(K | x_0) = \exp - \theta[\zeta(K) \cap \zeta(x_0)], \quad (7)$$

$$Q_2(K | x_0) = \exp - \int_{\zeta(x_0)} \theta(dy) [1 - e^{-\theta[\zeta(K) \cap \zeta(y)]}]. \quad (8)$$

with  $\zeta(K) = \cup \{ \zeta(z), z \in K \}$ . Relation (8) shows also that functional  $Q_n(K | x_0)$  converges rapidly toward an asymptotic value, as it involves an exponentiation more at each step. When daily local information will be available, Equations (6) to (8) will be able to serve to test the pertinence of the model, and if so, to short term forecast.

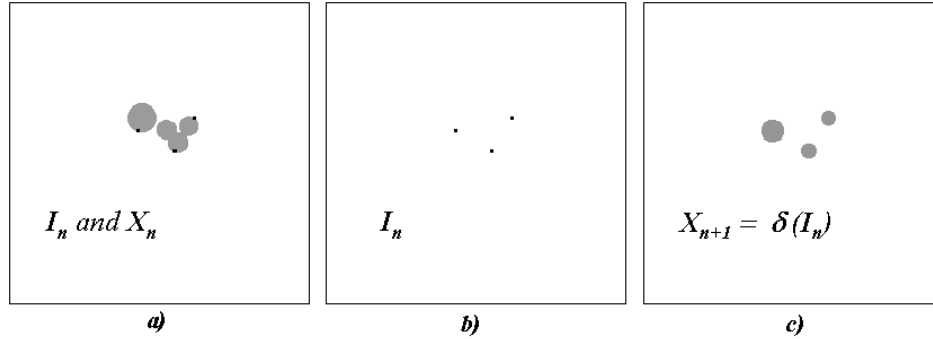


Figure 8: a) random spread  $X_n$  and random seats  $I_n$  at stage  $n$ ; b) seats  $I_n$  alone; c) random spread  $X_{n+1}$

### 3.3 SPONTANEOUS EXTINCTION

We now develop a second consequence of the random spread model, which is less demanding than a daily forecast, since local information is summed up over a long period. The fire which stems from a given point seat  $x_0$  may go out, spontaneously, after one, two, or more stages. The description of this phenomenon is the concerns of the whole space, and involves no particular compact set  $K$ . Denote by  $h(n | x_0)$  the probability that the fire extinguishes at most at step  $n$ . This event occurs before the second step when no Poisson point falls inside set  $\delta(x_0)$ , i.e. when

$$h(1 | x_0) = \exp\{-\theta[\delta(x_0)]\}. \quad (9)$$

Similarly, the probability of a spontaneous extinction before step  $n$  is given by the expression

$$h(n+1 | x_0) = \exp\{1 - \int_{\delta(z)} \theta(dy) h(n | y)\}. \quad (10)$$

Introduce the quantity

$$u(z) = \int_{\delta(z)} \theta(dx) \quad (11)$$

and suppose that

$$\mathbf{u} = \sup\{u(z), z \in \mathbb{R}^2\} < 1. \quad (12)$$

Then Relation (12) implies that  $h(n | x_0) \leq \mathbf{u}^n$ . The probability that the fire extinguishes spontaneously before step  $n+1$  decreases more rapidly than the geometrical sequence  $\mathbf{u}^n$ .

When  $\mathbf{u} \geq 1$ , the situation changes, and there is a non zero probability of an infinite propagation. Therefore, if  $Z$  stands for the set of all points where  $u(x) \geq 1$ , then there is every chance that the fire invades the connected component of  $\delta(Z)$  that contains point  $x_0$ .

Such a partition of the geographical space into connected zones where either  $\mathbf{u} < 1$  or  $\mathbf{u} \geq 1$  will serve to forecast the burnt areas in Selangor in Section 5.2.

#### 4. THE THREE PARAMETERS OF THE FIRE MODEL

Applying the random spread model to Selangor forest fires requires we firstly fix on the two input parameters  $\delta$  and  $\theta$ . We take  $\theta(x)$  proportional to  $f_w(x)$ , where  $f_w(x)$  is the fuel amount intensity at point  $x$  as depicted in Figure 4c, and take  $\delta(x)$  as equal to the disc of radius  $r(x)$ , where  $r(x)$  stands for the spread rate at point  $x$  (Figure 4c).

##### 4.1 Structuring function $\delta$ and rate of spread

The digital scale for  $r$ , in Figure 4a, is of 0.433 km/pixel. According to the Canadian forestry commission, the median value for a fire spread equals 0.6 metres/minute (Canadian Forestry, 1992), this number is of course the concern of Canadian forests, but it gives a likely order of magnitude for Malaysia. In the simulations below, the day is taken as the unit step of time, i.e. if set  $X$  is the fire at day  $n$ , then  $\beta(X)$  represents the fire at day  $(n+1)$ . Moreover, the following equalities hold inter-pixel distance/day =  $0.443 \times 10^3$  /1440 meter/minute = 0,307 m/mn.

Therefore the average rate of spread over the digital map  $r$  of Figure 4a must be  $\cong 2$  inter-pixel/day, which amounts to assign values 1 to 5 to the five grey levels of the map. The five possible values of  $r(x)$  generate the five discs  $\delta(x)$  of radii  $r(x)$  that are depicted in Figure 11.

##### 4.2 Intensity $\theta$ and fuel consumption

We also have to draw the Poisson intensity  $\theta$  from the available data. In the random spread  $\beta$ , this intensity reflects the propensity of a fire to occur. Physically speaking,  $\theta$  is thus proportional to the energy released by the fire develops. Such an amount is itself proportional to the fuel types of Figure 4b when each of them is weighted according to its own flammable value as indicated in Table 1, and depicted in Figure 4c. We can write

$$\theta(x) = k \cdot f_w(x) \quad x \in S \quad (13)$$

where  $S$  stands for Selangor state territory. The fuel consumption  $f_w$  has dimension of a weight/unit area, whereas  $\theta$  is a number/unit area, which implies dimension  $[\text{weight}]^{-1}$  for the coefficient  $k$ . For example, if the above flammable weights area expressed in tons per  $\text{m}^2$  then  $k$  is given in  $[\text{tons}]^{-1}$ . For a given choice of units, the numerical value of  $k$  may be estimated by matching the fire simulations with the actual burnt areas (see below). Note that function  $f_w$  differs from the total fuel consumption in the sense of the Canadian FBP model. The latter involves also time dependent parameters, such as moisture.

##### 4.3 Seasonal factor $k$

In Equation (13) the factor  $f_w$  corresponds to the permanent, or static, vegetal substratum for the fuel consumption, whereas all dynamic causes are regrouped in the factor  $k$ , constant over the space and which takes the meaning of a seasonal coefficient. Indeed, the Malaysian climate, where rainy and dry seasons alternate, makes the total number of high spots vary, as it can be observed in Figure 2. A specific fuel map for each season should

probably be more convenient for finer analyses. In the simplified approach of this paper, the degree of drought is completely transferred to the coefficient  $k$ , which takes different values according to the season, so that

$$\theta(x,t) = k(t) f_w(x). \quad (14)$$

The hot spots number allows us to estimate the seasonal factor involved in Relations (13) and (14). Selangor area  $a(S)$  is equal to 79,969 pixels, and the average number of Poisson points over the set  $S$  of Selangor is merely equal to 500. On the other hand, we draw from Table 1 that the sum of the fuel amount over  $S$  equals  $3 \times 49,637 + 4 \times (137,480 + 54,548) + 5 \times 62,665 = 304,130$  in dimensionless units. Therefore, by integrating Equation (13) over  $S$ , we find numerically

$$\int_S \theta(x) d(x) = 500 / 79,969 = k \int_S f_w(x) d(x) = 304,130 k / 79,969, \text{ from which we draw} \\ k = 1.64 \times 10^{-3} \quad (15)$$

## 5 RESULTS

In section 3, the fire front was modelled at each step  $i$  as the random spread  $X_i$ . We now consider the cumulative process  $Y_n(x_0)$ , from an initial point seat  $x_0$  to the  $n^{\text{th}}$  spread step  $X_n(x_0)$  i.e.

$$Y_n(x_0) = \cup \{ X_i(x_0), 1 < i \leq n \}. \quad (17)$$

$Y_n(x_0)$  is the region burnt by the fire after  $n$  steps, it is sometimes called scar by the forestry services. Figure 10b shows the scar due to the two successive spreads  $X_n$  and  $X_{n+1}$ .

Focusing on Selangor case, we will use the random spread model in two different manners, by performing simulations and by matching the theoretical prediction with the actual scars.

### 5.1. Scar simulations

We now simulate the scar obtained after five years of fires in Selangor, from year 2000 to 2004. To do so, we keep the same parameters as previously, i.e. the two maps Figure 4a and c, and the seasonal factor  $k$  of Rel. (15). It remains to choose an input seat. We will take all known hot spots during the period, i.e. the union of the three maps Figure 2a, b, and c, which results in Figure 12a. Clearly, most of these hot spots did not yield a fire. Nevertheless, it can be instructive to observe on simulations what can happen if we take all of them as inputs in the random spread model, and the variability of the possible scars they can induce.

Two simulations were computed by taking Figure 12a as common input  $I_0$ . They are depicted in Figure 12b and c, where the sets in black are obtained by taking the union of the nine stages of fire spread  $\delta(I_0) \dots \delta(I_8)$ . When higher terms are added to the union, the latter does not practically change, so that the simulation gives an estimate of the whole

scar. The shapes of the burnt zones are more regular in the simulations than in Figures 6b or 14b, because the chosen structuring function  $\delta$  is circular, but this could easily be improved.

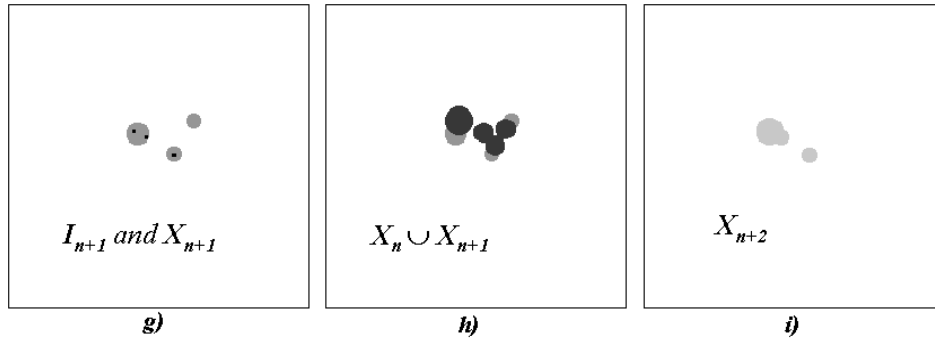


Figure 10: g) New seats  $I_{n+1}$  resulting of the intersection depicted in Figure 9; h) scar  $X_n \cup X_{n+1}$ ; i) new spread  $X_{n+1} = \delta(I_{n+1})$ .



Figure 11: Series of structuring functions for the five levels of the rate of spread map of Figure 4a.

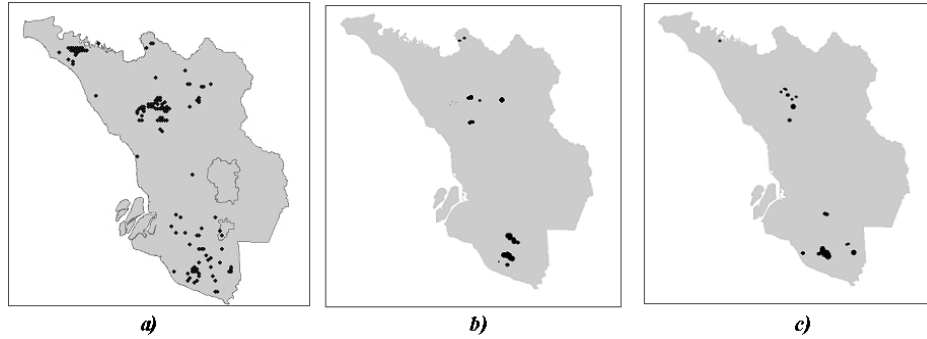


Figure 12: a) All hot spots detected between 2000 and 2004, b) and c) Two simulations of resulting scar regions .

### 5.2 Scar prediction

The results of Section 3.3 on the spontaneous extinction allow us to match the actual scars data with the behaviour of the model. The key parameter, here, turns out to be the product  $u(x)$  of Relation (9). In each region  $Z$  where all  $u(x)$ ,  $x \in Z$ , are noticeably  $\geq 1$ , any initial seat invades progressively the whole region, whereas in the regions with  $u(x) < 1$ , the spread stops by itself, all the sooner since  $u(x)$  is small. In Selangor's case, the expression of  $u$  from the two maps of Figure 4a and c is as follows

$$u(x) = \int \theta(z) 1_{\delta(x)}(z) dz = k \int f_w(z) 1_{\delta(x)}(z) dz \cong \pi k f_w(x) r^2(x). \quad (17)$$

This expression suggests to introduce the *scar function*  $s(x) = f_w(x) r^2(x)$ , as depicted in Figure 13.

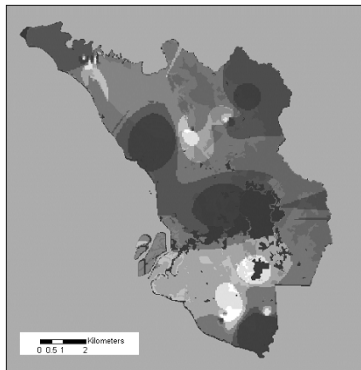


Figure 13: Scar function  $s = f_w \times r^2 = u / \pi k$  whose thresholds estimate the burnt scar zones.

This scar function  $s$  is accessible from the experimental data, since functions  $r$  and  $f_w$  are known from Figure 4a and 4c respectively. Note that map  $s$  is not obtained by simulations, but comes from a combination of the input parameters of the random spread model. By setting a threshold on image  $s$  at level  $1/\pi k$ , one splits the plane into the two regions where, either fires spontaneously extinguish (when  $s(x) < 1/\pi k$ ), or invade the connected components that contain their initial seats (when  $s(x) \geq 1/\pi k$ ).

For example, if we take for  $k$  the value  $1.64 \times 10^{-3}$  of Equation (15), and which corresponds to visually sound simulations, we obtain  $1/\pi k = 193.6$ . The two sets above thresholds 190 and 200 are depicted in Figure 14a, side by side with the burnt areas (Figure 14b). In Figure 14a, the fire locations A to E predicted by the model point out regions of actual burnt scars. Such a remarkable result could not be obtained from the maps  $f_w$  and  $r$  taken separately: the scare function  $s = f_w r^2$  means something more, which corroborates the random spread assumption. Region F is the only one which seems to invalidate the model. As a matter of fact this zone is occupied by peat swamp forest, or rather, was occupied. It is today the subject of a fast urbanization, linking the international airport of Kuala Lumpur to the administrative city of Putra Jaya. Several hot-spots are indicated in Figure 12a for this area, but one easily imagines that when seats start, they are immediately located and put out. Also, the rough fuel estimates of Table 1 should probably be refined. Nevertheless, on the whole, the random spread model turns out to be realistic.

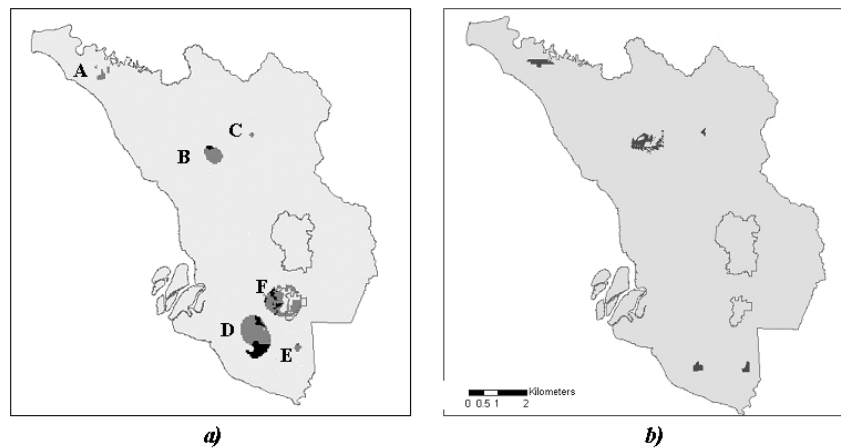


Figure 14: a) Two thresholds of function  $s$  for  $1/\pi k=190$ , in dark grey, and  $1/\pi k=200$ , in black (the simulations suggest value 193); b) map of the actual burnt areas. Note the similarity of the sets, and of their locations.

## 6 VARIANTS

Here are a few variants, just sketched, of the previous random spreads.  $I_{n+1} = \beta(I_n)$

### 6.1. Burning crowns

For the sake of simplicity, and also for keeping down the number of parameters, we supposed in section 3 that the seats  $I_{n+1}$  at stage  $n+1$  were all included in the dilates by  $\delta$  of the seats  $I_n$ . As a matter of fact, the assumption is not essential at all, and we can as well restrict the new seats  $I_{n+1}$  in crowns around the seats  $x \in I_n$ .

### 6.2 Time dependent spreads

Suppose that the conditions of the phenomenon under study vary according to the time, and that steps 1, 2, 3, and so on, represent day (or week, or month) 1, 2, 3, and so on. If the two maps  $\delta$  and  $\theta$  are actualised, i.e. if we have  $\delta_n$  and  $\theta_n$  at day, week, or month  $n$ , then  $X_2, X_3$ , etc. are obtained from the maps of the corresponding time units. The two relations (1) and (3) become

$$X_{n+1} = \cup \{ \delta_n(x_k), x_k \in I_n \}$$
$$I_{n+1} = \cup \{ \delta_n(x_i) \cap P_i(\theta_n), x_i \in I_n \}$$

In addition, new "initial" phenomena may appear at every step. One may have at day  $n$  the propagation of the previous fires, plus some new hot spots,  $H_n$  say. The sequence becomes

$$I'_n = I_n \cup H_n$$
$$X'_{n+1} = \cup \{ \delta_n(y_k), y_k \in I_n \cup H_n \}$$

etc..

### 6.3 Superimpositions

The above variants describe relatively local propagations. However, in Malaysian peat swamp forests, fire propagates also by the underground, from a distance, and reappears elsewhere after some time (Wan Ahmad, 2002). In Mediterranean forests, the fires send away burning pieces of wood that generate new hot spots (Carrega, 2002; Coli and Al 2002). These two particular modes may be added to the model, by taking two pairs  $(\delta, \theta)$  instead of one and by inserting the second pair either at each step  $X_n$  (Mediterranean mode), or in the passage  $X_n \rightarrow X_{n+p}$ , for a given integer  $p > 0$  (Malaysian mode). If the two modes are supposed to act independently, then the Q functional of their union (Rel. (5)) is simply the product of the Q functionals of each term.

## 7 CONCLUSION

The random spread model provides a tool for understanding forest fire propagation. It proved to be able to predict most of the burnt zones of Selangor. Some aspects of fire spread are well handled by the theory (e.g. short term fire evolution, Relation (6), or its probability of extinction, Equation (12), or again the function  $g$  of the burnt areas).

However long term prediction is the only part of the model that the above study validates, by showing that the theoretical results coincide with the actual burnt areas. But one can reach others aspects by computing simulations. For example, by multiplying simulations which use the same hot spot input, as in Figure 13, one obtains average estimates of the size distributions, and the evolution of the burnt areas day after day. The model may also serve to compare different input maps of fuel consumption and spread rates, and to measure which ones fit the best with the actual burnt zones.

Just as any stochastic model, that of random spread lies on a series of assumptions. All land parameters are supposed to be exhaustively summarized in the two spread rate map and fuel map. The propagation from a seat is supposed to be isotropic, which is an approximation. Relief, proximity of roads, and other local factors surely intervene (Setiawan and Al, 2004). Also, the basic assumptions of the model do ignore a possible interaction between fire propagation and human actions for extinguishing it. Similarly, the model is not adapted to fires that are deliberately lighted for destroying a forest, day after day, according to a fully deterministic plane.

The type of approach suggested by forest fires propagation turns out to be more general. We focused here on a unique variable, but one could also try and evaluate the impact of forest fire on other forest features, relevant to ecosystem and biodiversity. Such multivariable interactions can easily be introduced in the formalism, either in a parallel way (intersection of parameters), or sequentially (conditionally to such event, such other event occurs). Several types of maps would have to be known, which risks limiting, in practice, the range of possibilities. And, of course, forest fires are not the only natural phenomena that spread more or less randomly. One can also think to the ways that mammals, insects, mushrooms, or plants, use to take over territories, or even to passive spreads such as those of pollutants.

## ACKNOWLEDGEMENTS

The authors would like to thank The Cilix Corp. for having allowed them to use their maps of fuel combustion and spread rate.

## REFERENCES

1. ABDULLAH, M.J., IBRAHIM, M.R., AND ABDUL RAHIM A.R. (2002), The incidence of forest fire in Peninsular Malaysia: History, root causes, prevention and control. *Workshop on prevention and control of fire in peatland, Kuala Lumpur, Malaysia, 19-21 March 2002*
2. ADB (Asian Development Bank) and BAPPENAS (National Development Planning Agency) (1999). Causes, extent, impact and costs of 1997/98 fires and drought. Final Report, Annex 1 and 2. Planning for Fire Prevention and Drought Management Project. *Asian Development Bank TA 2999-INO July 1998 -- March 1999*. Fortech, Pusat Pengembangan Agribisnis, Margueles Pöyry. Jakarta, Indonesia.
3. BAK, P. CHEN, K., AND PACZUSKI M. (2001) Solitons in the one-dimensional forest fire model, *Physical Review Letters, The American Physical Society*, vol. 86 n°11, March 2001.
4. BLANCHI, R., JAPPIOT, M. AND ALEXANDRIAN, D. (2002), Forest fire risk assessment and cartography. A methodological approach. *Forest Fire Research and Wildland Fire Safety*, Viegas Ed. Millpress Rotterdam.

5. CARREGA, P. (2002), Relationship between wind speed and the rate of spread of a fire front in field conditions : an experimental example from the Landes forest. *Forest Fire Research and Wildland Fire Safety*, Viegas Ed. Millpress Rotterdam.
6. W.R. CATCHPOLE, E.A. CATCHPOLE, A.G. TATE, B. BUTLER, R.C. ROMMEL (2002), A model for the steady spread of fire through a homogeneous fuel bed. *Forest Fire Research and Wildland Fire Safety*, Viegas Ed. Millpress Rotterdam, 2002.
7. COLIN, COLIN, P.-Y., AND AL., 2002. Saltus program-spot fires: knowledge and modelling, in *Proc. of the IV international conf. on Fire Research*, Luso, Portugal, 2002.
8. CRISP (2001). Remote Sensing of Land/Forest Fires. [http://www.crisp.nus.edu.sg/forest\\_fire/fire.html](http://www.crisp.nus.edu.sg/forest_fire/fire.html) [4 July 2001].
9. ESRI (2006). *ArcGIS 9, Using ArcGIS Desktop*. Environmental Systems Research Institute, Redlands.
10. FORESTRY CANADA FIRE DANGER GROUP, (1992) Development and Structure of the Canadian Forest Fire Behaviour Prediction System *Information Report ST-X-3*, Forestry Canada, Ottawa..
11. GANTZ, D., (2002) *framing Fires: a country-by-country analysis of forest and land fires in the ASEAN nations*. World Conservation Union.
12. HAIRI SULIMAN, M.D., SERRA, J. AWANG M.A.( 2005) Morphological Random Simulations of Malaysian Forest Fires, in *DMAI/2005*, X. Chen Ed., AIT Bangkok.
13. MAHMUD, M. (1999) Forest Fire Monitoring And Mapping In South East Asia *National Seminar On LUCC and GOF (NASA/EOC)*, 12 Nov. 1999, Bangi Selangor Malaysia.
14. MAAROF, A.H., (2002). Fire prevention and protection in peat swamp areas: Pahang experience. *Proceedings of the workshop on prevention and control of fire in peatlands*, 21-30. 19-21 March, Kuala Lumpur, Malaysia.
15. MATHERON, G. (1975) *Random sets and integral geometry*, Wiley, New-York,
16. QIANG, M., AND BRAODHEAD, J.S. (2002) An Overview of Forest Products Statistics in South and Southeast Asia. *Information and Analysis for Sustainable Forest Management: Linking National and International Efforts in South and Southeast Asia* (Qiang, M. & J.S. Braodhead, eds.). Food and Agriculture Organization of the United Nations, Bangkok.
17. SEAFDRS (2003). *Southeast Asia Fire Danger Rating System Manual*, Canadian Forest Service, Alberta, Canada.
18. SERRA, J. (1982) *Image analysis and mathematical morphology*, Academic Press, London.
19. SERRA, J. (2007) The Random Spread Model, *Mathematical Morphology and its Applications to Image and Signal Processing*, G. Banon, J. Barrera, and U.M. Braga-Neto, Eds, Ministério da Ciência e Tecnologia , Brasil, 87-100.
20. SÉRO-GUILLAUME, O. AND MARGERIT, J. (2002) Modelling forest fire: Part I: a complete set of equations derived by extended irreversible thermodynamics. *Int. Journal of Heat and Mass Transfer* 45, 1705-1722.
21. SETIAWAN, I., MAHMUD, A.R., MANSOR, S. MOHAMED SHARIF, A.R., AND NURUDDIN, A.A. (2004) GIS-grid-based and multi criteria analysis for identifying and mapping peat swamp forest fire hazard in Pahang, Malaysia. *Disaster prevention and management* Vol. 13, N° 5 , 379-386.
22. VAN WAGNER (1987). Development and Structure of the Canadian Forest Fire Weather Index System. Forestry Technical Report 35. Canadian Forestry Service, Ottawa, Ontario
23. WAN AHMAD, W. S. (2002) Forest Fire Situation in Malaysia, *IFFN*, 26, 66-74.
24. ZHANG, Y.-H., WOOSTER, M.J., TUTUBALINA, O. AND PERRY, G.L.W. (2003) Monthly burned area and forest fire carbon emission estimates for the Russian Federation from SPOT VGT, *Remote Sensing of Environment*, 87, 1-15.